Anomaly in the viscosity of liquid KCl at high pressures

Yoshio Kono,[1] Curtis Kenney-Benson,[1] Changyong Park,[1] Guoyin Shen,[1] and Yanbin Wang[2]

[1]*High Pressure Collaborative Access Team (HPCAT), Geophysical Laboratory, Carnegie Institution of Washington, 9700 S. Cass Avenue, Argonne, Illinois 60439, USA*

[2]*GeoSoilEnviroCARS, Center for Advanced Radiation Sources, The University of Chicago, 5640 S. Ellis Avenue, Chicago, Illinois 60637, USA*

We measured viscosity of KCl and NaCl liquids up to 7.3 GPa and observed a clear discontinuity in the pressure dependence of viscosity for liquid KCl at around 2 GPa. The viscosity of liquid KCl increased rapidly at 1.5–2.2 GPa, above which it remained virtually constant. Structural data of KCl liquid also showed a pronounced change signified by the ratio r_2/r_1, where r_1 and r_2 are the nearest- and the second-neighbor distances, respectively. In contrast, both viscosity and the r_2/r_1 ratio changed linearly with pressure for liquid NaCl. Our observation suggests that viscosities of KCl and NaCl liquids strongly correlate with the structural changes in terms of the r_2/r_1 ratio. The viscosity anomaly in liquid KCl is found to be at pressures close to that of the B1-B2 transition in solid KCl.

Pressure-induced structural changes and associated physical properties in liquids are among the most fundamental and challenging topics in condensed matter physics. Pressure-induced structural transition has been studied both experimentally and theoretically in several liquids, such as phosphorus,[1] nitrogen,[2] silicon,[3] selenium,[4] tellurium,[5] and water.[6] In contrast to the extensive studies on liquid structures, however, physical property changes accompanied by the liquid structural change have not yet been well investigated. Although some anomalous behavior has been reported in physical properties of liquids accompanied by the structural transitions,[7–11] clear correlations between physical properties and the structural characteristics are still lacking. In this paper, we report experimental results of viscosity changes in liquid KCl and liquid NaCl at high pressures. It has been known that liquid KCl undergoes a structural transition around 2 GPa,[12] while liquid NaCl shows continuous increase in coordination number with increasing pressure to 5 GPa.[13] In correlation with the structural transition, we observed a viscosity anomaly in liquid KCl, while liquid NaCl showed a normal continuous increase of viscosity up to 7.3 GPa.

Viscosity is one of the most fundamental transport properties in liquid. Extensive studies have been made at ambient pressure using various techniques (cf. a review of Ref. 14). However, the effect of pressure on the viscosity of liquids remains poorly understood partly due to the lack of experimental data. High-pressure falling-sphere viscometry was first developed in an effort to measure viscosities of molten earth materials.[15–22] These measurements were confined to highly viscous materials due to the limited imaging rate (typically 30–60 frames per second (fps) and up to 125 fps) in common x-ray radiography apparatus. As a consequence, it was difficult to investigate low-viscosity liquids such as metals[23] and salts[24] whose viscosities are around 1 mPa·s or less at ambient pressure. Some studies report viscosities in the 4–20 mPa·s range for iron alloys[18,19] using falling-sphere velocities determined based on only 2–4 images. This limited imaging rate makes it difficult to ensure that the falling sphere has reached terminal velocity and results in large uncertainties in the calculated viscosity. Rutter *et al.*[20] determined low

viscosities (of around 2.4–4.8 mPa·s) by adopting a sphere having similar density to that of the liquid sample in order to decrease terminal velocity. The drawback of this approach is that small uncertainties in the liquid density lead to large relative changes in the density difference between the liquid and the probing sphere, causing a large uncertainty in viscosity determination. For instance, a calculation reveals that a 3% uncertainty in the liquid density results in more than 34% uncertainty in the viscosity determination. Since Rutter *et al.* did not measure liquid density and viscosity simultaneously, uncertainties in liquid density could be a significant source of errors in their reported viscosity. To overcome this limitation and to precisely determine the viscosities of low-viscosity materials at high pressures, we have adopted a high-speed camera (Photron FASTCAM SA3) that can collect images of falling spheres at a rate of more than 1000 fps.

Our combined liquid structure and falling-sphere viscometry measurements were conducted in a Paris-Edinburgh cell[25,26] at 16-BM-B beamline of the High Pressure Collaborative Access Team (HPCAT) at the Advanced Photon Source. We used a cell assembly similar to that of Sakamaki *et al.*[27] with cylindrical samples, typically 2 mm in diameter and 2 mm in height. Each sample was enclosed in a BN capsule at the center of the cell assembly. Pt balls roughly 100 μm in diameter were used as probing spheres. In all experiments, the probing spheres fell immediately upon melting of KCl and NaCl, due to their low viscosities. Therefore, both viscosity and structure were measured at temperatures just above melting, and our results represent the pressure dependence of viscosities of KCl and NaCl liquids along the melting curves (Fig. 1). Pressures were determined by the equation of state of MgO.[28] For the calculation of pressures, we used temperatures estimated from power-temperature relation curves that were determined in a separate experiment using an identical cell configuration. The estimated temperatures were consistent with the melting curves of KCl[29] or NaCl[30] with uncertainties less than $\pm 5\%$ (Fig. 1).

Falling-sphere viscometry measurements were carried out by x-ray radiography using the high-speed camera. The pixel size of the high-speed camera (5.92 $\pm$ 0.01 μm/pixel) was
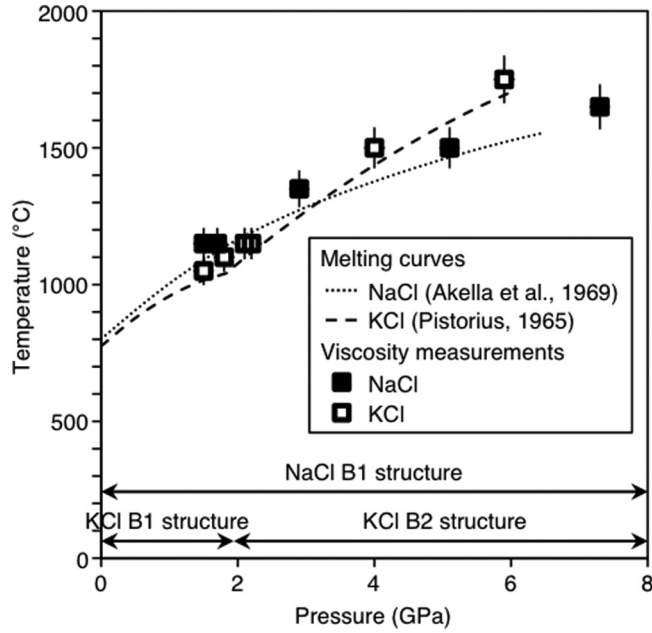
FIG. 1. Pressure and temperature conditions of viscosity measurements shown with melting curves of KCl (Ref. 29) and NaCl (Ref. 30). Bottom arrows indicate crystal structures of KCl and NaCl at the pressure conditions. It is known that solid KCl undergoes B1-B2 transition at 1.9 GPa (Ref. 41), while solid NaCl has B1 structure to 30 GPa (Ref. 42).

calibrated by using a 497-μm WC ball as a scale reference. We used two Pt spheres in each experiment: one placed at the top of the sample to measure velocity of the probing sphere over the longest travel distance possible and another located near the center of the sample to identify melting of the sample and to trigger the high-speed camera. This two-ball approach was necessary because the sphere at the top of the sample was hidden by the top WC anvil at high pressures. In addition, falling of the Pt sphere over the longest distance is important to achieve terminal velocity. A series of falling-sphere images was recorded at 2000 fps with an exposure time of 0.5 ms.

Figure 2(a) shows a series of images representing the falling Pt sphere with time in liquid NaCl at 2.9 GPa and around 1350 °C (see movie in Supplemental Material[31]). We analyzed the position of the Pt sphere in each frame by using the Tracker plug-in in ImageJ software. The excellent linearity in the sphere travel distance with time indicates that terminal velocity (v) was achieved [Fig. 2(b)]. The viscosity (η) was calculated with the Stokes equation, including the correction factors for the effect of the wall (F)[32] and for the end effect (E)[33]

$$\eta = \frac{g d_s^2 (\rho_s - \rho_l)}{18 v} \frac{F}{E}, \tag{1}$$

$$F = 1 - 2.104 \left(\frac{d_s}{d_l}\right) + 2.09 \left(\frac{d_s}{d_l}\right)^3 - 0.95 \left(\frac{d_s}{d_l}\right)^5, \tag{2}$$

$$E = 1 + \frac{9}{8}\frac{d_s}{2Z} + \left(\frac{9}{8}\frac{d_s}{2Z}\right)^2, \tag{3}$$

where ρ and d are density and diameter, with subscripts s and l denoting properties of probing spheres and liquid, respectively. Z is the sample height. The diameter of the
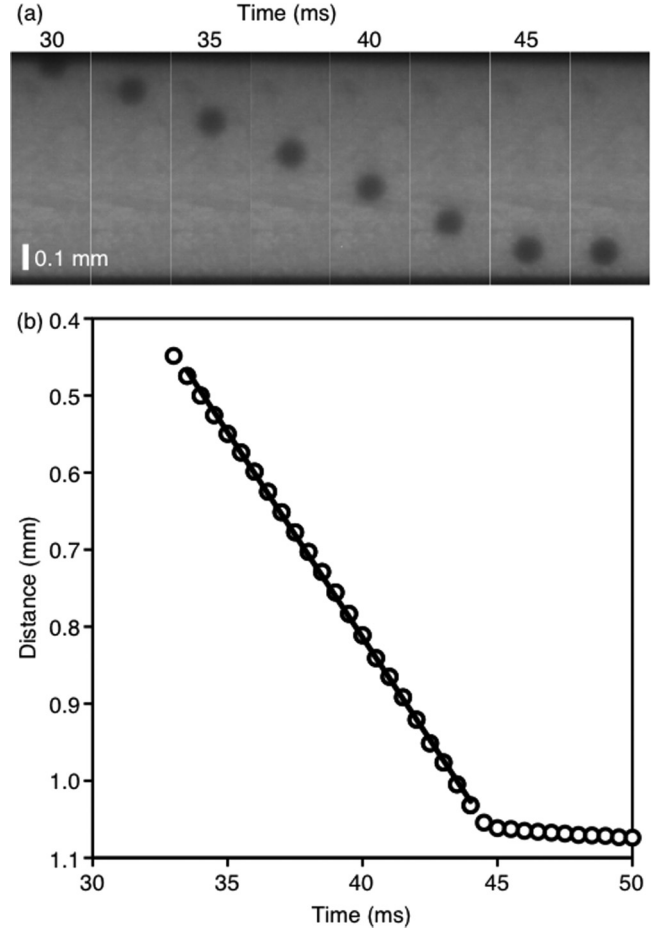

FIG. 2. X-ray radiography images of falling Pt sphere (106 μm in diameter) in liquid NaCl at 2.9 GPa and ~1350 °C (a) and the results of the falling distance analysis for each frame (b). The constant slope before the sphere reaches the bottom confirms that terminal velocity was measured with substantial oversampling.

Pt spheres was measured by x-ray radiography using the high-resolution camera.[34] The diameter of the sample was assumed to be same as the initial sample diameter (2 mm), because it was difficult to determine the boundary between the liquid sample and the BN capsule due to the lack of contrast with white x-ray radiography and hence to measure the diameter of the sample at various pressure and temperature conditions. This assumption does not give significant influence on the determination of viscosity. A calculation showed that a 10% difference in sample diameter would cause only a 1% difference in the Faxén factor F and the resultant viscosity. For the Pt spheres (94–133 μm) used in this study, values of F were 0.86–0.90. In addition, we calculated the end-effect factor ($1/E$) by equating the distance between the top and bottom WC anvils to the parameter Z, yielding $1/E$ values between 0.87 and 0.94. The density of the spheres was calculated by the equation of state for platinum.[35] For densities of the liquids, however, we used those of liquid NaCl (1.547 g/cm^3) and liquid KCl (1.518 g/cm^3) at ambient pressure and 817 °C and 787 °C, respectively,[24] because liquid densities at high pressures and high temperatures corresponding to our experimental conditions have not been reported. The use of constant liquid densities does not significantly influence the viscosity
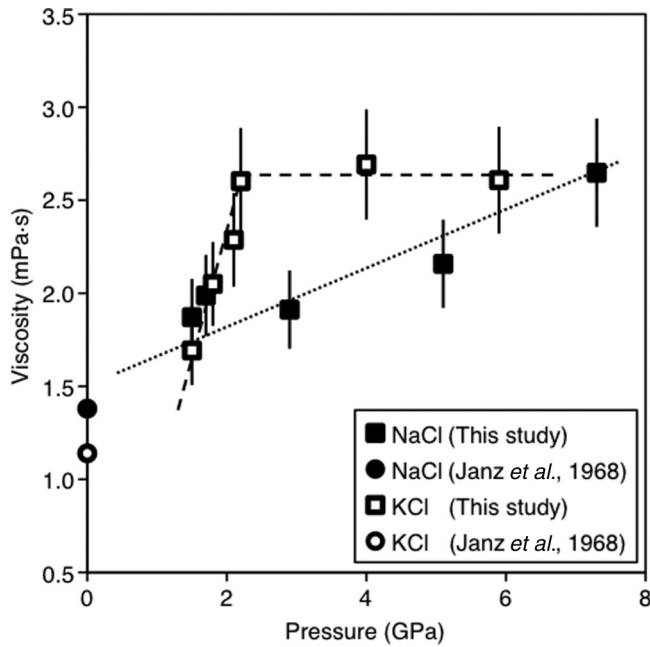
FIG. 3. Viscosity of liquid KCl and liquid NaCl as a function of pressure up to 7.3 GPa along the melting curves. The dashed and dotted lines are guides for eyes. Vertical bars represent uncertainty of our viscosity measurement of $\pm 11\%$.
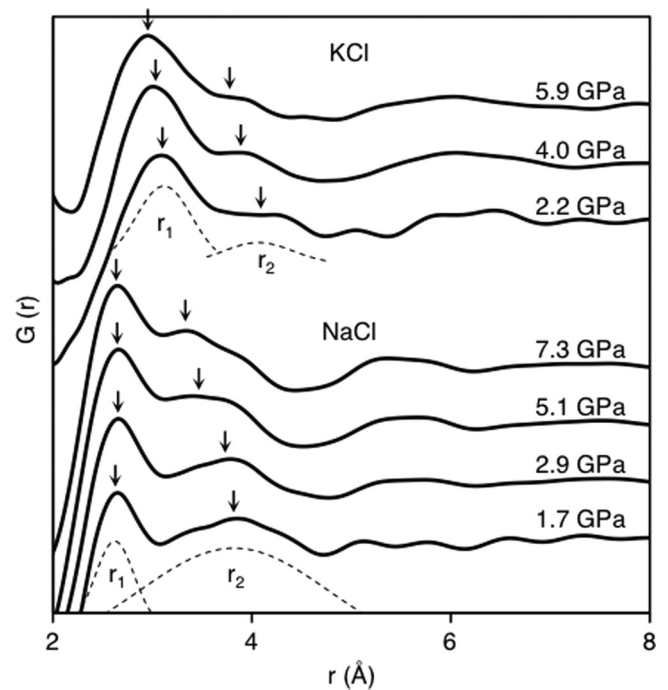

FIG. 4. The reduced pair distribution function $G(r)$ of liquid KCl and liquid NaCl at high pressures. The first peak of $G(r)$ in liquid KCl or liquid NaCl represents the nearest-neighbor cation-anion distance (r_1), and cation-cation or anion-anion distances (r_2) appear as a broad hump following the first peak. Examples of the peak-position fit to a Gaussian curve for the $G(r)$ of the liquid KCl at 2.2 GPa and that of the liquid NaCl at 1.7 GPa are shown by the dashed lines. Arrows indicate shift of the r_1 and r_2 peak positions with respect to variation of pressure.

determination because of the large difference in densities between Pt (e.g., 21.45 g/cm^3 at ambient condition) and the liquids. For example, a 10% difference in liquid density would only change the viscosity by 0.8%. In contrast, it has been pointed out that the uncertainties in terminal velocity play a dominant role in the precision of the viscosity determination.[36] In this study, terminal velocities were accurately determined with standard deviations of ± 2.5–6.5%. Due to the small sphere size used in our experiment, uncertainty in the diameter of the probing sphere also contributes to errors in viscosity. Our high-resolution x-ray radiography setup had a ± 2-μm resolution in imaging, corresponding to up to about $\pm 3.5\%$ uncertainty in the resultant viscosity. We therefore conclude that the overall uncertainty in our viscosity determination is less than $\pm 11\%$.

Figure 3 shows viscosities of KCl and NaCl liquids as a function of pressure along the melting curves. At ambient pressure, the viscosities of both liquids are similar[24] and remain so up to 1.5 GPa (Fig. 3). Above this pressure, viscosities of KCl and NaCl liquids display different behaviors. Viscosity of liquid NaCl almost linearly increases with increasing pressure to 7.3 GPa. In contrast, the viscosity of KCl increases significantly at 1.5–2.2 GPa so that by 2.2 GPa the viscosity (2.7 mPa·s) is 57% higher than that at 1.5 GPa (1.7 mPa·s), which is significantly larger than the uncertainties in measurement. Above 2.2 GPa, the viscosity of KCl liquid remains virtually constant to 5.9 GPa. The distinct kink in the viscosity of liquid KCl is in stark contrast to the linear increase in viscosity of liquid NaCl with increasing pressure up to 7.3 GPa.

Interestingly, the viscosity anomaly of liquid KCl observed in this study is in clear correlation with the structural change of liquid KCl reported in Urakawa *et al.*[12] In order to

clarify the viscosity-structure correlation, we also measured the structures of KCl and NaCl liquids *in situ* at high pressures immediately after each viscosity measurement. These structural measurements were conducted using the multiangle energy-dispersive x-ray diffraction (EDXD) technique,[37] by collecting diffraction patterns at 2θ angles of 3°, 4°, 5°, 7°, 9°, 11°, 14°, 18°, 23°, and 29°. Analysis of the obtained EDXD data was based on a software package by Funakoshi.[38] The structural measurements at low pressures for KCl (1.5, 1.8, and 2.1 GPa) and NaCl (1.5 GPa) liquids were not successful, because liquid samples leaked during the long data collection required for the structure measurements (around 2.5 h) probably due to insufficient sealing of the thin BN capsule at low-pressure conditions. All other structure measurements at higher pressures up to 7.3 GPa were successful.

Figure 4 shows the reduced pair distribution function $G(r)$ of KCl and NaCl liquids at high pressures. Previous ambient pressure measurement showed that for liquid NaCl the r_1 and r_2 distances are 2.6 and 3.8 Å, respectively,[39] and those of liquid KCl are 3.05 and 4.35 Å, respectively.[40] At high pressures, our $G(r)$ results show well-resolved r_1 peaks, whereas broad r_2 peaks appear broader, particularly in liquid NaCl. In addition, the data show some ripples that are strongly dependent on the maximum Q range included in the Fourier transformation to determine $G(r)$ (see Fig. S1 in Supplemental Material[31]). In particular, the r_2 peak lost its shoulders with decreasing maximum Q range, becoming a single broad peak. Therefore,
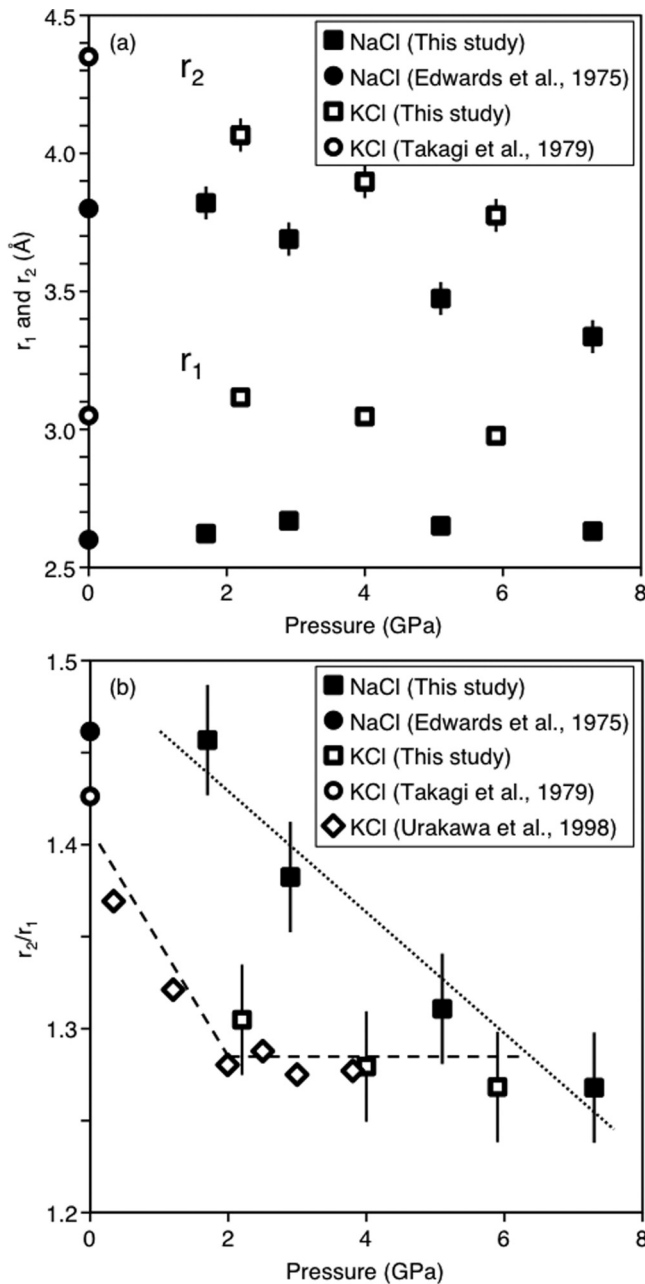
FIG. 5. Pressure dependence of the nearest- (r_1) and the second-neighbor (r_2) distances (a) and the ratio (r_2/r_1) (b) of liquid KCl and liquid NaCl. The dashed and dotted lines are guides eyes for liquid KCl and liquid NaCl, respectively. Vertical bars represent uncertainty of the r_2/r_1 ratio of ± 0.03.

± 0.02 Å for the r_1 and ± 0.06 Å for the r_2. Uncertainties of the resultant r_2/r_1 ratio were less than ± 0.03.

Figure 5 displays pressure dependence of the r_1 and r_2 distances, and the ratio r_2/r_1 of KCl and NaCl liquids, together with literature data.[12,39,40] The r_2/r_1 ratios of liquid KCl obtained in this study are consistent with those of Urakawa *et al.*[12] at pressures above 2 GPa. The data of Urakawa *et al.*[12] show a distinct change in the pressure dependence of the r_2/r_1 ratio of liquid KCl at ~ 2 GPa, in close correlation with our observed viscosity behavior (Fig. 3). The r_2/r_1 ratio rapidly decreases with increasing pressure below ~ 2 GPa[12] and then becomes nearly constant above ~ 2 GPa (Fig. 5). In contrast, the r_2/r_1 ratio of liquid NaCl continuously decreased with increasing pressure in the pressure range of this study.

Overall, the comparison between the viscosity and structural changes clearly shows that viscosities of both liquid KCl and liquid NaCl strongly correlate with the r_2/r_1 ratio (Fig. 3 and Fig. 5). The viscosities of liquid KCl and liquid NaCl vary inversely with the change of the r_2/r_1 ratio as a function of pressure. The r_2 distance continuously decreases in both liquid KCl and liquid NaCl with increasing pressure regardless of constant viscosity in liquid KCl or increase of viscosity in liquid NaCl. In contrast, the r_1 distance shows different behavior in liquid KCl than in liquid NaCl. The r_1 distance of liquid NaCl is nearly constant (2.62–2.67 Å) up to 7.3 GPa, while that of liquid KCl showed a slight decrease from 3.12 Å at 2.2 GPa to 2.98 Å at 5.9 GPa. Thus, the different variation of the r_2/r_1 ratio between two liquids at high pressures is mainly attributed to the difference in the high-pressure behavior of the r_1 distance. Because the r_1 distance is a direct measure of the coordination numbers of these liquids, the observed viscosity anomaly at 2 GPa for KCl reflects a strong correlation between the macroscopic behavior and the microscopic coordination number change.[12]

in the peak-fitting process, we assumed two peaks below ~ 5 Å and fit each peak with its own Gaussian curve to determine their shifts with respect to pressure (Fig. 4). Uncertainties in the peak positions were determined from three sigma of the standard deviation of each Gaussian curve fitting, typically at

[1]Y. Katayama, T. Mizutani, W. Utsumi, O. Shimomura, M. Yamakata, and K. Funakoshi, Nature (London) **403**, 170 (2000).

[2]B. Boates and S. A. Bonev, Phys. Rev. Lett. **102**, 015701 (2009).

[3]N. Funamori and K. Tsuji, Phys. Rev. Lett. **88**, 255508 (2002).

[4]K. Tsuji, J. Non-Cryst. Solids **117–118**, 27 (1990).

[5]N. Funamori and K. Tsuji, Phys. Rev. B **65**, 014105 (2001).

[6]A. K. Soper and M. A. Ricci, Phys. Rev. Lett. **84**, 2881 (2000).

[7]Y. Katayama, Y. Inamura, T. Mizutani, M. Yamakata, W. Utsumi, and O. Shimomura, Science **306**, 848 (2004).

[8]M. Krisch, P. Loubeyre, G. Ruocco, F. Sette, A. Cunsolo, M. D'Astuto, R. LeToullec, M. Lorenzen, A. Mermet, G. Monaco, and R. Verbeni, Phys. Rev. Lett. **89**, 125502 (2002).

[9]Y. Katayama, K. Tsuji, H. Kanda, H. Nosaka, K. Yaoita, T. Kikegawa, and O. Shimomura, J. Non-Cryst. Solids **205–207**, 451 (1996).

[10]V. V. Brazhkin, M. Kanzaki, K.-i. Funakoshi, and Y. Katayama, Phys. Rev. Lett. **102**, 115901 (2009).

[11]V. V. Brazhkin, I. Farnan, K.-i. Funakoshi, M. Kanzaki, Y. Katayama, A. G. Lyapin, and H. Saitoh, Phys. Rev. Lett. **105**, 115701 (2010).

[12]S. Urakawa, N. Igawa, O. Shimomura, and H. Ohno, in *Properties of Earth and Planetary Materials at High Pressure and Temperature, Geophysical Monograph 101*, edited by M. H. Manghnani and T. Yagi (American Geophysical Union, Washington, D.C., 1998), pp. 241–248.

[13]S. Urakawa, N. Igawa, O. Shimomura, and H. Ohno, Am. Mineral. **84**, 341 (1999).

[14]R. F. Brooks, A. T. Dinsdale, and P. N. Quested, Meas. Sci. Technol. **16**, 354 (2005).

[15]I. Kushiro, H. S. Yoder, Jr., and B. O. Mysen, J. Geophys. Res. **81**, 6351 (1976).

[16]S. K. Sharma, D. Virgo, and I. Kushiro, J. Non-Cryst. Solids **33**, 235 (1979).

[17]M. Kanzaki, K. Kurita, T. Fujii, T. Kato, O. Shimomura, and S. Akimoto, in *High Pressure Research in Minetal Physics*, edited by M. H. Manghani and Y. Shono (Terrapub, Tokyo, 1987), pp. 195–200.

[18]D. P. Dobson, W. A. Crichton, L. Vocadlo, A. P. Jones, Y. Wang, T. Uchida, M. Rivers, S. Sutton, and J. P. Brodholt, Am. Mineral. **85**, 1838 (2000).

[19]H. Terasaki, T. Kato, S. Urakawa, K.-i. Funakoshi, A. Suzuki, T. Okada, M. Maeda, J. Sato, T. Kubo, and S. Kasai, Earth Planet. Sci. Lett. **190**, 93 (2001).

[20]M. D. Rutter, R. A. Secco, H. Liu, T. Uchida, M. L. Rivers, S. R. Sutton, and Y. Wang, Phys. Rev. B **66**, 060102 (2002).

[21]H. Terasaki, A. Suzuki, E. Ohtani, K. Nishida, T. Sakamaki, and K. Funakoshi, Geophys. Res. Lett. **33**, L22307 (2006).

[22]J.-P. Perrillat, M. Mezouar, G. Garbarino, and S. Bauchau, High Pressure Res. **30**, 415 (2010).

[23]T. W. Chapman, AIChE J. **12**, 395 (1966).

[24]G. J. Janz, F. W. Dampier, G. R. Lakshminarayanan, P. K. Lorenz, and R. P. T. Tomkins, Natl. Stand. Ref. Data Ser. (US, Natl. Bur. Stand.) **15**, 1 (1968).

[25]J. M. Besson, R. J. Nelmes, G. Hamel, J. S. Loveday, G. Weill, and S. Hull, Physica B **180–181**, 907 (1992).

[26]S. Klotz, G. Hamel, and J. Frelat, High Pressure Res. **24**, 219 (2004).

[27]T. Sakamaki, Y. Wang, C. Park, T. Yu, and G. Shen, J. Appl. Phys. **111**, 112623 (2012).

[28]Y. Kono, T. Irifune, Y. Higo, T. Inoue, and A. Barnhoorn, Phys. Earth Planet. Inter. **183**, 196 (2010).

[29]C. W. F. T. Pistorius, J. Phys. Chem. Solids **26**, 1543 (1965).

[30]J. Akella, S. N. Vaidya, and G. C. Kennedy, Phys. Rev. **185**, 1135 (1969).

[31]See Supplemental Material at http://link.aps.org/supplemental/10.1103/PhysRevB.87.024302 for the original movie of the images shown in Fig. 2(a); see Fig. S1 of this Supplemental Material for the effect of the maximum Q range on the determination of G(r).

[32]H. Faxén, Ann. Phys. (Paris) **373**, 89 (1922).

[33]A. D. Maude, Br. J. Appl. Phys. **12**, 293 (1961).

[34]Y. Kono, C. Park, T. Sakamaki, C. Kenny-Benson, G. Shen, and Y. Wang, Rev. Sci. Instrum. **83**, 033905 (2012).

[35]P. I. Dorogokupets and A. Dewaele, High Pressure Res. **27**, 431 (2007).

[36]M. Brizard, M. Megharfi, and C. Verdier, Metrologia **42**, 298 (2005).

[37]A. Yamada, Y. Wang, T. Inoue, W. Yang, C. Park, T. Yu, and G. Shen, Rev. Sci. Instrum. **82**, 015103 (2011).

[38]K. Funakoshi, Ph.D. thesis, Tokyo Institute of Technology, 1997.

[39]F. G. Edwards, J. E. Enderby, R. A. Howe, and D. I. Page, J. Phys. C **8**, 3483 (1975).

[40]R. Takagi, H. Ohno, and K. Furukawa, J. Chem. Soc., Faraday Trans. 1 **75**, 1477 (1979).

[41]S. N. Vaidya and G. C. Kennedy, J. Phys. Chem. Solids **32**, 951 (1971).

[42]W. A. Bassett, T. Takahashi, H.-K. Mao, and J. S. Weaver, J. Appl. Phys. **39**, 319 (1968).